

Redesigned NIF Capsule Increases Viability of Ge-Doped CH as Ablator.

NIF ignition capsules have been designed with ablators of polyimide, beryllium, and doped CH. Of these three, the original material—doped CH—appeared in simulations to be the most susceptible to hydrodynamic instability growth. The original design was optimized for implosion margin, which emphasized high implosion velocity and left the target susceptible to short-wavelength instability growth. Improved calculational capability over the years since then has proven that the original design could only tolerate perturbations smaller than about 30-nm rms roughness. In contrast, more recent designs using polyimide can tolerate about 50-nm roughness, and beryllium about 60-nm, all at 1.3-MJ laser energy absorbed and nominal hohlraum coupling efficiency.

Because doped CH is probably the easiest material from which to fabricate the capsules, we have revisited the optimization of the doped CH capsules. The figure shows a full scan of the space of possible capsule dimensions, representing optimization of 333 different designs. The laser energy and hohlraum coupling

are held fixed in the scan over capsule dimensions. In order to scan the space completely and efficiently, a computer routine was written that automatically finds the optimal pulse shape for each design. The contours of 1D yield show the full operating space for these capsules, bounded by ablator burnthrough on the left and inadequate implosion velocity on the upper right. Two-dimensional simulations are in progress to find the optimum design that includes hydrodynamic instability growth. A first result is indicated: a target with thicker fuel can tolerate considerably larger perturbations than could the original design. Similar detailed optimization will be done for the polyimide and beryllium capsules.

Sub-picosecond Proton Moiré Interferometry Demonstrated Using Laser-Produced MeV Proton Beams.

When light or particles pass through a pair of transmission gratings whose rulings are rotated with respect to each other, a series of Moiré fringes will be observed, as shown in Figure 1. The inclination of these fringes depends on the degree of collimation of the source, and this has been widely used in optics to measure the focal length of lenses. While diffraction theory must be used to analyze optical Moiré patterns, diffraction can be neglected for particles, allowing simple geometric considera-

tions to be used for interpretation of the proton Moiré patterns, greatly simplifying the analysis of experimental results.

Figure 2 shows images of a laser-generated proton beam obtained in a recent experiment carried out on the JanUSP laser at LLNL, in collaboration with physicists from V division and Queens University, Belfast. Proton Moiré fringes can clearly be seen in the location where the sub-picosecond pulse of 6-MeV protons has passed through the crossed transmission gratings. The orientation of the fringes was consistent with a point

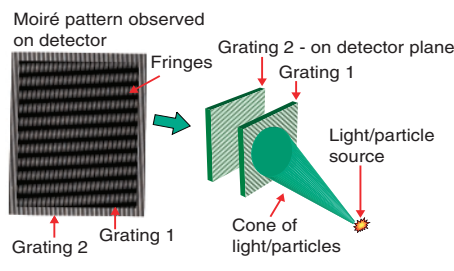
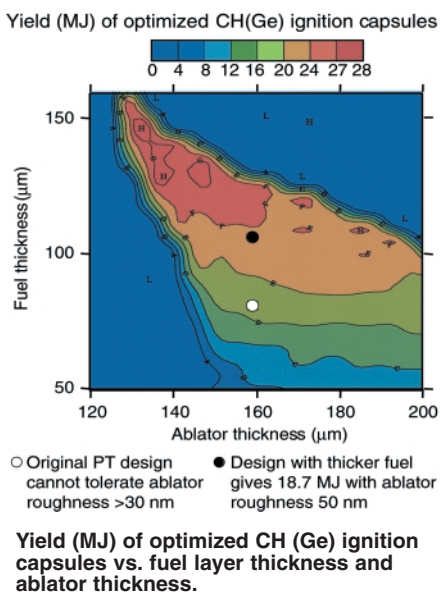


Figure 2. Images on film of a laser-generated proton beam produced by focusing the 100-fs JanUSP laser onto a thin target at an intensity of $1 \times 10^{20} \text{ Wcm}^{-2}$. (a) Image through transmission gratings and (b) image through hole in grating substrate.

source of protons located within 2 mm of the 5-cm distant laser-irradiated target surface.

These experiments represent an essential proof-of-principle result because in a direct analogy with optical experiments, shifts in these Moiré fringes can be used to locally measure angular deflections in the proton beam. A quantitative measurement of these deflections may allow us to infer the magnitude of extremely large electric fields in plasmas with picosecond time resolution.

Formation and Symmetry Control of Fuel Layers in a NIF-Scale Hohlraum.

We have made the first good D_2 ice layers in a hohlraum and have demonstrated ability to control the symmetry of these layers. The ice layer grows on the inside of a 2-mm-diameter plastic shell suspended in a NIF-scale hohlraum. A ring of infrared (IR) laser power is projected through each laser entrance hole and is scattered off the carefully prepared, nearly Lambertian hohlraum wall (Figure 1). The D_2 is symmetrically redistributed inside the shell by absorption of the uniformly scattered IR power. The shadowgraph image of the ice layer at the hohlraum midplane has an rms roughness of $8\text{ }\mu\text{m}$ (Figure 2). Neglecting the lowest two modes gives a $2.6\text{-}\mu\text{m}$ rms roughness that approaches the NIF smoothness require-

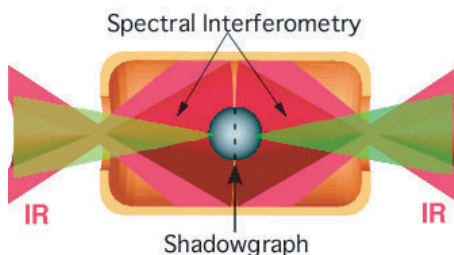


Figure 1. Infrared heating and characterization of fuel layers in hohlraums.

ment of $1\text{-}\mu\text{m}$ rms. The amplitude of the first two azimuthal modes can be reduced by optimizing the IR alignment. Spectral interferometry and shadowgraph ice thickness measurements are used to optimize the IR pointing and side-to-side power balance. The measured ice response to IR tuning is reproduced in a complete ray-tracing and thermal model of this experiment. With this successful demonstration of IR layering in a

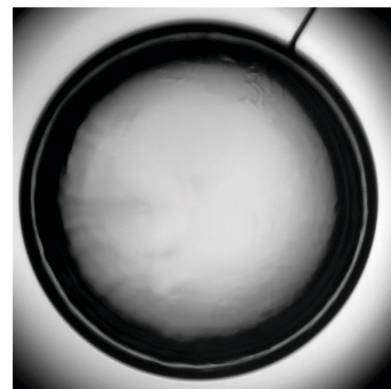


Figure 2. Shadowgraph image of D_2 fuel layer formed in a hohlraum.

hohlraum, future experiments will now focus on slower growth to reach NIF smoothness requirements, as previously demonstrated in capsules inside integrating spheres. This work is done in collaboration with General Atomics and Schafer Corporation.

Efficient, >10 keV X-Ray Source Production.

Efficient, bright, laser-produced x-ray sources at photon energies above 6 keV are a challenge to produce because convective and soft x-ray radiative losses incurred with solid targets limit the plasma temperature. Nevertheless, hard x-ray sources are essential for future experiments at NIF, many of which

require such sources for radiography between 10 and 20 keV.

To address this need and others, recent experiments performed in collaboration with Q Division and the Naval Research Laboratory at the OMEGA laser in Rochester, NY, have demonstrated creation of 13-keV photons at near 1%

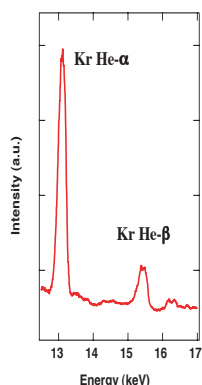


Figure 1. Time-integrated He-like Kr spectrum from a 0.5 atm gas-filled target.

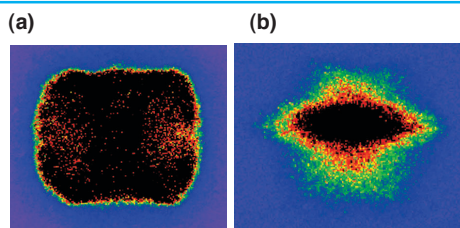


Figure 2. (a) X-ray image at 0.8 ns showing full target diameter of 1.5 mm and length of 1.2 mm in emission. (b) X-ray image at 1.8 ns; same scale as previous image, but emission is localized on axis.

efficiency using 0.5–2 atm Kr gas-filled low-Z cylinders. The gas is supersonically heated by forty $0.35\text{-}\mu\text{m}$ wavelength, 1-ns square laser beams to produce He-like ions that radiate K-shell emission over millimeter dimensions (see Figures 1 and 2). Previous work on gas-filled Xe and Ar targets has shown an order of magnitude gain in 3–6 keV x-ray conversion efficiency over disk targets, and also that K-shell emitters can be more efficient than L-shell emitters for equivalent electron temperature. Kr gas was chosen to take advantage of these properties. Targets filled with 0.5 to 2.0 atm of Kr gas produce conversion

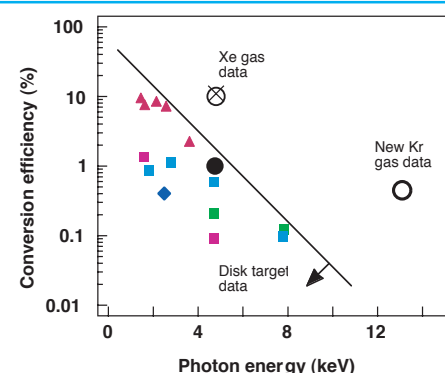
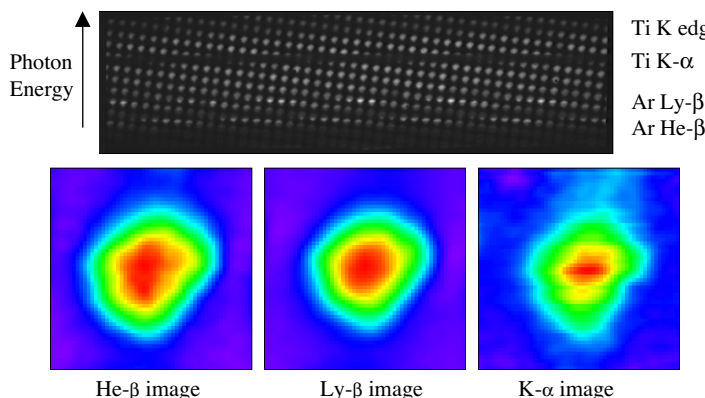


Figure 3. X-ray conversion efficiency from gas-filled targets (open symbols) and disk targets (filled symbols) irradiated with $0.35\text{-}\mu\text{m}$ laser light. New Kr gas data is ~2 orders of magnitude above the projected disk x-ray conversion efficiency.

efficiencies from 0.3 to 0.6%, which represent at least a 100× improvement in conversion efficiency at 13 keV over what is predicted for solid targets (see Figure 3). Surprisingly, the lowest fill produces the highest conversion efficiency. This is ascribed to compression of the lower-fill Kr plasmas by the inwardly ablating cylinder walls, prolonging the emission after laser heating.

Monochromatic X-Ray Imaging—a New Tool for Diagnosing Plasma Conditions.

Multispectral imaging is a powerful tool for the quantitative diagnosis of three-dimensional structure in plasmas. This technique uses multiple monochromatic x-ray images, obtained over a band of x-ray wavelengths, to infer information about temperature and density gradients within the plasma. We recently implemented a multispectral x-ray imaging diagnostic on the OMEGA laser at the University of Rochester's Laboratory for Laser Energetics (UR-LLE), and used it to obtain data on temperature and density gradients within indirect-drive implosion cores for the first time. We also obtained preliminary data on areal density modulations within the pusher. The diagnostic,



Typical MMI2 data from an indirect-drive implosion of a capsule containing Ar-doped D₂ gas surrounded by Ti-doped plastic. Core density and temperature gradients can be inferred from comparison of images obtained in the He-β and Ly-β spectral bands, while pusher areal density modulations can be inferred from comparison of images taken within the Ti K-α band to images taken just outside this band.

the MMI2, uses an array of pinholes mounted on the target to produce hundreds of individual core images; it is modeled after a concept developed at UR-LLE. A multilayer Bragg mirror placed between the pinhole array and the CID (charge-injection device) detector effectively monochromatizes the

individual images at an x-ray energy related to the local angle of incidence upon the mirror. The result is an x-ray spectrum made up of individual core images. The images provide information about spatial structure, and the spectral dispersion provides temperature and density information.

Simulations Show Value of Imaging Down-Scattered Neutrons on NIF Ignition Implosions.

For some years, efforts have been under way to image the neutrons emitted from ICF implosions. These images have utilized the 14-MeV neutrons from the DT reaction and have provided an image of hot burning fuel. Recent simulations have explored the value of imaging the down-scattered neutrons that are produced by scattering at approximately 90° in the relatively cool high-density fuel surrounding the central hot spot. Imaging the high-

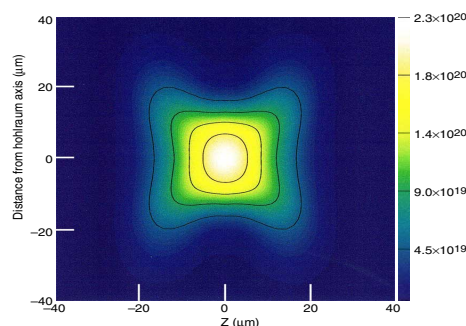


Figure 1. Image of 14-MeV primary neutrons from a simulated implosion of a NIF ignition target, with a P_6 perturbation causing spikes along the hohlraum waist and 30° from the axis. The perturbations were large enough to prevent ignition, bringing the yield down from 17 MJ to 50 kJ.

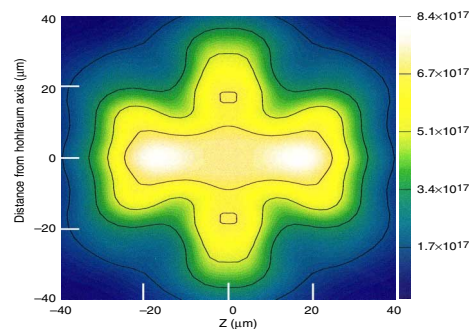


Figure 2. Image of 6- to 7-MeV neutrons from the same implosion. These neutrons have scattered at about 90° in the high-density fuel regions around the hot spot.

density fuel is likely to be very valuable in attempts at ignition, since the sources of nonuniformity in the implosion often result in variations in the density and location of this material. The nature of these variations will be important indicators of the source of nonuniformity. Figures 1, 2, and 3 illustrate the value of this technique. All three are simulated neutron images, with 10-μm resolution, of a baseline cryogenic ignition implosion. Figures 1 and 2 are of the same implosion, which had a sixth order Legendre polynomial perturbation. The perturbation was large enough to prevent ignition, with yield 50 kJ instead of the nominal

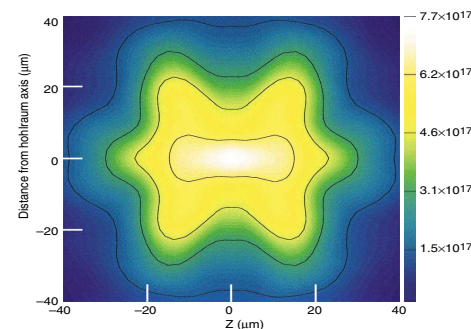


Figure 3. Image of 6- to 7-MeV neutrons from a simulation with the opposite sign of the P_6 perturbation.

17 MJ. Spikes penetrated the hot spot along the hohlraum waist and at 30° from the axis. Figure 1, showing the image of the primary 14-MeV neutrons, shows little of this structure; only the innermost part of the hot spot burned enough to produce significant brightness. Figure 2 shows the image of 6- to 7-MeV neutrons and clearly shows the high-density DT features on the waist and surrounding the axis. Figure 3 shows another simulation in which the sign of the perturbation was reversed, so that the spikes are penetrating along the pole and at 60°. The high-density spikes are clearly evident, and the complementarity to Figure 2 is striking.

For comments about content of the *Bimonthly Update*, contact Bruce A. Hammel (925) 422-3299.

To get on the mailing list of the *LLNL ICF Program Bimonthly Update and Annual Report* send a request to miguel1@llnl.gov. These reports and other LLNL ICF Program information are available on our Web page at <http://www.llnl.gov/nif/icf.html>. This work was performed under the auspices of the U.S. Department of Energy by University of California Lawrence Livermore National Laboratory under Contract W-7405-Eng-48.

Prototype Ignition Target Successfully Filled in the D₂ Test System.

All current designs of indirect-drive ignition targets for the National Ignition Facility (NIF) include cryogenic solid-fuel layers in the target capsule. These targets require special cryogenic support equipment. We have recently successfully tested some critical scientific prototypes of this equipment. Because many of the ignition capsules would burst if filled to the required pressures, they must be cooled to cryogenic temperatures before they are removed from their fill cells, and then maintained at these low temperatures until shot. Our tests consisted of inserting an assembled indirect-drive target, including a capsule in a hohlraum with thin polymer windows over the laser entrance holes (LEH),



Figure 1. The assembled target is covered by a cold shroud.

into a fill cell, diffusion filling the capsule to 400 atmospheres with deuterium without breaking the thin LEH windows, and cooling the target after fill. The target was then removed from the cold fill cell by attaching it to a specially designed cryostat. The target, with

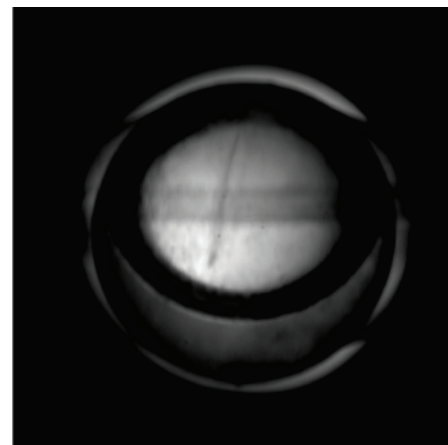


Figure 2. The capsule, viewed through a window in the hohlraum, is partially filled with liquid deuterium.

the filled capsule, seen in Figure 1, was maintained in this cryogenic state for several days. This is the first demonstration of these crucial steps for fielding indirect-drive ignition targets. Its success adds technical confidence to the design concept of the NIF cryogenic target systems.

X-Ray Radiography of Direct-Drive Implosions on the OMEGA Laser.

A capability has been developed on the OMEGA laser to simultaneously implode a capsule in a direct-drive configuration while acquiring two nearly orthogonal images of the implosion via x-ray radiography. The implosion is driven using 40 of OMEGA's 60 beams; the remaining beams are used to illuminate a pair of backlighter foils with 10 beams each. The energy of the 40 drive beams can be adjusted to produce either a symmetrical implosion (Figure 1) with 2% rms illumination nonuniformity or a nonideal implo-

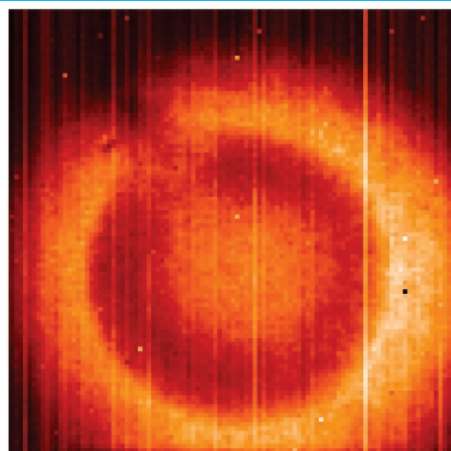


Figure 1. Symmetrically driven implosion.

sion (Figure 2) with a slowly changing and controlled 5:1 variation in drive uniformity around the 1120-μm-diameter capsule. This data is

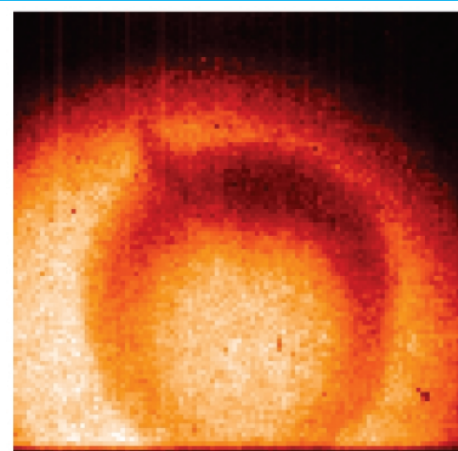


Figure 2. Nonideal driven implosion.

useful for validating the performance of numerical codes when there is departure from ideal symmetry.

CVD Diamond as a Current-Mode Detector for Neutron Spectroscopy at NIF

Thermonuclear fusion in deuterium-deuterium (DD) and deuterium-tritium (DT) fuel generates fast primary-reaction neutrons with energies of 2.5 and 14 MeV, respectively. The detailed energy spectrum of neutrons escaping from a compressed inertial confinement fusion (ICF) capsule includes information about the temperature of the central hot spot through thermal Doppler broadening of the primary reaction peak, and information about the areal density of cold fuel surrounding the hot spot through scattering, which slows primary neutrons to lower energies. For these reasons, neutron spectroscopy is a critical ICF diagnostic and will be vital for the ignition campaign on the National Ignition Facility (NIF).

The most straightforward technique for ICF neutron spectroscopy is “time-of-flight.” With this technique, the variation in neutron energies gives rise to a spread in arrival times at a distant neutron detector. By recording the neutron current as a function of time (current-mode detection), the neutron energy spectrum can be inferred by knowing the distance between the target and the detector.

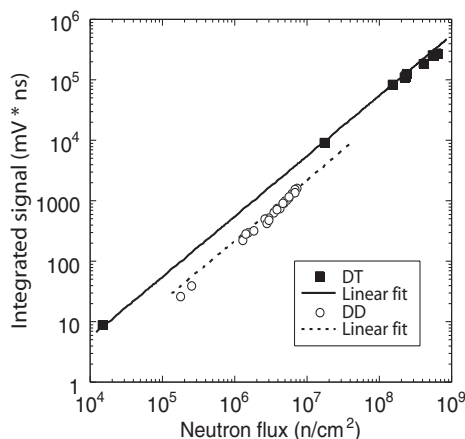


Figure 2. CVD diamond signal vs neutron flux for DD and DT neutrons at OMEGA (neutron flux determined using standard scintillator diagnostic).

We are examining various current-mode detectors for operation as neutron time-of-flight (NTOF) spectrometers inside the NIF target chamber, and the most promising of these is chemical vapor deposition (CVD) diamond. Diamond, well known for its short response time and radiation hardness, is well suited for the in-chamber NTOF application. Synthetic CVD diamond is chosen over natural diamond because it can be purchased in larger, cheaper and more sensitive wafers, but natural diamond and other materials may play a role in higher-yield NIF experiments.

We have fielded CVD diamond detectors for neutron spectroscopy

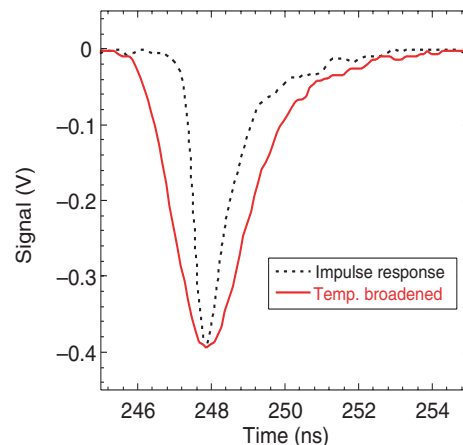


Figure 3. Temporal broadening of CVD diamond neutron signal for a DD shot at OMEGA. Deduced ion temperature is 7.2 keV. This agrees well with the 7.1-keV result from standard OMEGA diagnostics.

applications at the University of Rochester’s Laboratory for Laser Energetics (LLE) OMEGA Laser Facility, in preparation for their use on NIF. These detectors were fabricated by LLNL using commercial CVD diamond wafers (see Figure 1). For operation inside the OMEGA target chamber, three different generations of housing designs have been fielded, with the latest demonstrating an average noise floor of ~3 mV. We are working on techniques to further reduce the noise floor by better subtraction of electromagnetic noise effects. So far, neutron tests at OMEGA (done in collaboration with LLE scientists) have demonstrated linear operation over 5 orders of magnitude in incident flux (Figure 2), as well as secondary-to-primary ratios and ion temperature measurements (Figure 3) in agreement with standard OMEGA scintillator diagnostics.

With continued successful development efforts at OMEGA, we expect CVD diamond to be a valuable ICF ignition diagnostic for neutron spectroscopy.



Figure 1. The original CVD diamond detector housing fabricated at LLNL.

Response of Materials during High-Pressure Shock Studied with X-Ray Diffraction

Scientists from the ICF Program at LLNL are working with researchers at the University of California, San Diego (UCSD) and the University of Oxford to study the response of materials during shock loading. The focus of this effort is to use in-situ dynamic x-ray diffraction to measure the response of the lattice structure directly. This technique uses x-rays to probe the lattice orientation and spacing by diffracting from the lattice as it compresses. The x-rays are diffracted from specific lattice planes according to the Bragg condition. As the material is compressed, the lattice spacing and orientation change, as indicated for the (111) planes of a cubic structure in Figure 1. As a result, the angle at which x-rays diffract changes.

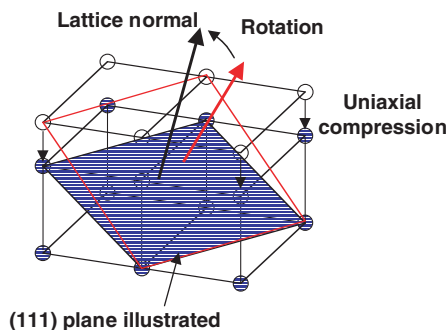


Figure 1. Schematic illustrating the change in lattice spacing and direction due to a uniaxial compression.

A new instrument was developed and fielded on target shots at the OMEGA laser. This is a large-angle coverage film detector that records x-rays diffracted from a large number of lattice planes simultaneously. It

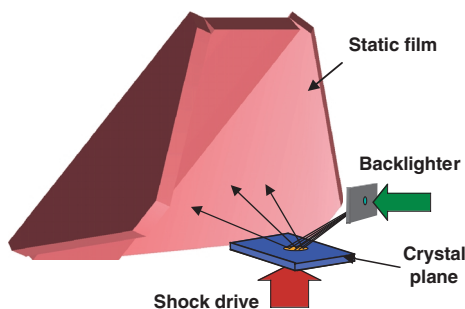


Figure 2. The large-angle detector consists of three film holders positioned to collect x-rays diffracted from the single crystal target at a wide range of angles.

consists of three film holders that are positioned around the target, collecting x-rays over a π -steradian solid angle (Figure 2). This instrument provides a capability to record the response of many different lattice planes simultaneously. Information from these different lattice planes allows us to infer the lattice configuration, even if a phase transformation occurs under shock loading.

The film images from one experiment are shown in Figure 3, displayed

in angle coordinates. Here, x-rays diffracted from a single crystal sample of Si are shown. The axes are ϕ and θ corresponding to the direction of the x-rays that are diffracted from the single crystal sample. The x-ray wavelength was 1.85 \AA . The target sample was compressed by direct laser irradiation along the (001) direction, with a peak pressure of approximately 16 GPa.

The film data from the shocked Si experiment shows diffraction lines from both the initial (uncompressed) and the shocked lattice on the left side of the figure. A simulated diffraction pattern is overlaid on the right side of the figure. By recording many lattice planes both parallel and oblique to the shock propagation direction, we obtain information on the lattice configuration during shock loading. In this case, all of the compressed lattice diffraction lines are matched by modeling with a 6% uniaxial compression.

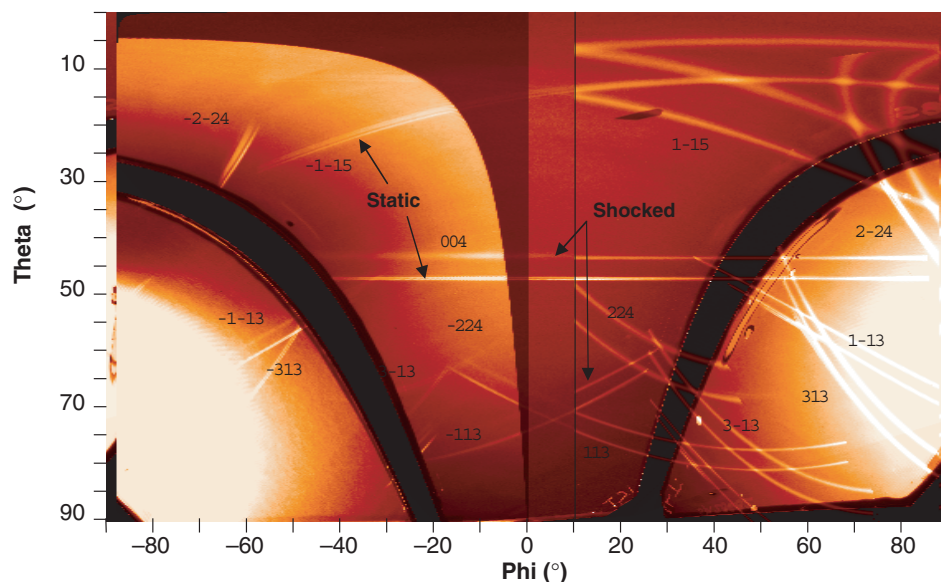


Figure 3. Film from one experiment showing 1.85 \AA x-rays diffracted from a $40\text{-}\mu\text{m}$ -thick single silicon crystal.